11-1-2013

# Insights Into the Carboxyltransferase Reaction of Pyruvate Carboxylase From the Structures of Bound Product and Intermediate Analogs

Adam D. Lietzan
*Marquette University*, adam.lietzan@marquette.edu

Martin St. Maurice
*Marquette University*, martin.stmaurice@marquette.edu

Accepted version. *Biochemical and Biophysical Research Communications*, Vol. 441, No. 2 (November 2013): 377-382. DOI. 

# Insights into the Carboxyltransferase Reaction of Pyruvate Carboxylase from the Structures of Bound Product and Intermediate Analogues

Adam D. Lietzan
*Department of Biological Sciences, Marquette University*
*Milwaukee, WI*
Martin St. Maurice
*Department of Biological Sciences, Marquette University*
*Milwaukee, WI*

**Abstract:** Pyruvate carboxylase (PC) is a biotin-dependent enzyme that catalyzes the MgATP- and bicarbonate-dependent carboxylation of pyruvate to oxaloacetate, an important anaplerotic reaction in central metabolism. The carboxyltransferase (CT) domain of PC catalyzes the transfer of a carboxyl group from carboxybiotin to the accepting substrate, pyruvate. It has been hypothesized that the reactive enolpyruvate intermediate is stabilized through a bidentate interaction with the metal ion in the CT domain active site. Whereas bidentate ligands are commonly observed in enzymes catalyzing reactions proceeding through an enolpyruvate intermediate, no bidentate interaction has yet been observed in the CT domain of PC. Here, we report three X-ray crystal structures of the *Rhizobium etli* PC CT domain with the bound inhibitors oxalate, 3-hydroxypyruvate, and 3-bromopyruvate. Oxalate,

*Biochemical and Biophysical Research Communications*, Vol. 441, No. 2 (November 2013): pg. 377-382. DOI. 

a stereoelectronic mimic of the enolpyruvate intermediate, does not interact directly with the metal ion. Instead, oxalate is buried in a pocket formed by several positively charged amino acid residues and the metal ion. Furthermore, both 3-hydroxypyruvate and 3-bromopyruvate, analogs of the reaction product oxaloacetate, bind in an identical manner to oxalate suggesting that the substrate maintains its orientation in the active site throughout catalysis. Together, these structures indicate that the substrates, products and intermediates in the PC-catalyzed reaction are not oriented in the active site as previously assumed. The absence of a bidentate interaction with the active site metal appears to be a unique mechanistic feature among the small group of biotin-dependent enzymes that act on α-keto acid substrates.

**Keywords:** biotin-dependent carboxylase, carboxyltransferase, pyruvate carboxylase

# Introduction

Pyruvate carboxylase (PC; EC 6.4.1.1) is a multifunctional, biotin-dependent enzyme that catalyzes the bicarbonate- and MgATP-dependent carboxylation of pyruvate to oxaloacetate, an important anaplerotic reaction in central metabolism (reviewed in [1]). Aberrant enzyme activities and protein expression levels are associated with Type II diabetes, tumor cell proliferation, and bacterial virulence. In all eukaryotes and most prokaryotes, PC is a homotetramer, with each monomer consisting of four functional domains: the biotin carboxylase (BC) domain, the carboxyltransferase (CT) domain, the biotin carboxyl carrier protein (BCCP) domain and the central allosteric domain. The catalytic reaction requires a covalently tethered biotin cofactor, which is initially carboxylated in the BC domain with the hydrolysis of MgATP. Following carboxylation, carboxybiotin physically translocates to the CT domain where the carboxyl group is transferred to pyruvate to form oxaloacetate.

While the reaction mechanism for the BC domain of PC has been extensively investigated, detailed insights into the CT domain reaction have only recently emerged. For example, the CT domain of *Rhizobium etli* PC (*Re*PC) utilizes a conserved Thr882 to shuttle a proton from pyruvate to the biotin enolate [2], while Arg548, Gln552, and Arg621 serve to stabilize the enolpyruvate intermediate [3,4], and Asp590 and Tyr628 form a substrate-induced biotin binding pocket to

*Biochemical and Biophysical Research Communications*, Vol. 441, No. 2 (November 2013): pg. 377-382. DOI. 

accommodate the insertion of carboxybiotin into the active site [5]. Recent X-ray crystal structures of PC have shown pyruvate bound in the active site [5–7] but, surprisingly, pyruvate does not coordinate the active site metal through a bidentate interaction. This unexpected pyruvate binding pose raises questions about the role of the metal ion in the carboxyltransferase reaction. A structure of the product, oxaloacetate, bound in the active site would further clarify the position of reactants relative to the active site metal ion. However, attempts at determining a structure of PC with bound oxaloacetate have not been successful, largely due to the relatively rapid rate of spontaneous oxaloacetate decarboxylation [5,6].

Here we report three X-ray crystal structures of the CT domain from *Re*PC with bound analogs of the reaction intermediate and product (Figure 1). The structure with oxalate, a stereoelectronic mimic of the enolpyruvate intermediate, suggests that the metal center does not directly participate in the reaction mechanism. Taken together with the structures of the CT domain with the product analogs, 3-hydroxypyruvate and 3-bromopyruvate, these structures contribute new details to the mechanistic description of the PC catalyzed reaction.

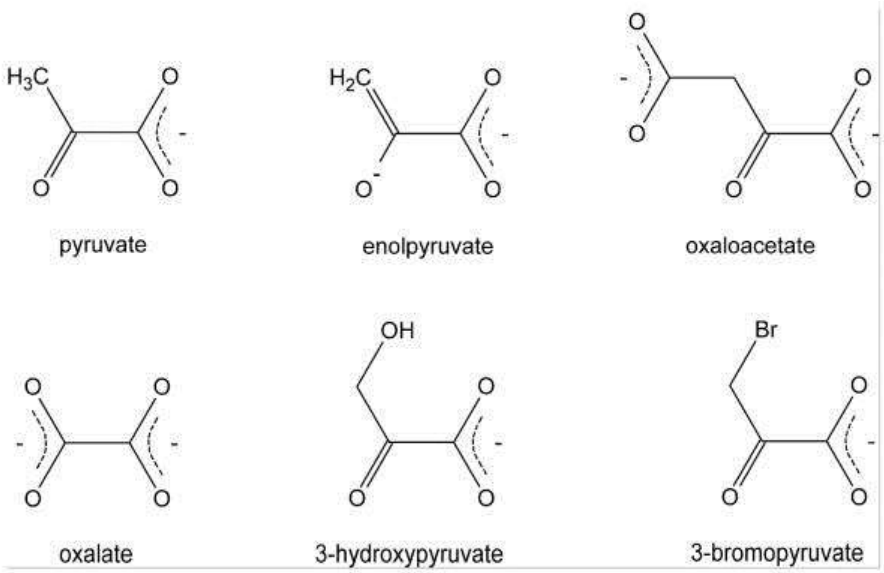


**Figure 1** Structures of the reaction substrate (pyruvate), reaction intermediate (enolpyruvate), reaction product (oxaloacetate), reaction intermediate analog (oxalate), and two reaction product analogs (3-hydroxypyruvate and 3-bromopyruvate).

*Biochemical and Biophysical Research Communications*, Vol. 441, No. 2 (November 2013): pg. 377-382. DOI. 

# Materials and Methods

## *General*

Oxalate and 3-bromopyruvate were purchased from Alfa Aesar. All other materials, including 3-hydroxypyruvate, were purchased from Sigma-Aldrich. ΔBCΔBCCP *Re*PC was previously subcloned into a modified pET-28a vector for recombinant expression in λ(DE3) lysogenized *Escherichia coli* BL21Star [5].

## *Protein Purification*

ΔBCΔBCCP *Re*PC protein was purified and concentrated as previously described [5].

## *Isothermal Titration Calorimetry*

ITC experiments were performed using a Microcal ITC200 (GE Life Sciences) with 296 μM ΔBCΔBCCP *Re*PC in 20 mM HEPES buffer (pH 7.5) in the ITC cell. This was titrated with 10 mM pyruvate or 3 mM oxalate in 20 mM HEPES buffer (pH 7.5). The binding isotherm was calculated after subtracting a control titration into an ITC cell containing 20 mM HEPES buffer (pH 7.5). Binding isotherms were fit to a one site binding model.

## *Protein Crystallization*

### *ΔBCΔBCCP RePC co-crystallization with oxalate*

ΔBCΔBCCP *Re*PC was crystallized using the batch crystallization method under oil, as previously described [5]. Crystallization conditions for the three crystal structures were nearly identical. For the ΔBCΔBCCP *Re*PC structure containing oxalate, the protein solution consisting of 10 mg/mL ΔBCΔBCCP *Re*PC and 25 mM oxalate was mixed at a 1:1 ratio with the precipitant solution comprised of 11.3% (w/v) PEG 8000, 99 mM BisTris (pH 6.0), and 346 mM tetramethylammonium chloride (TMACl). A seed stock was generated using the seed bead kit from Hampton Research (Aliso Viejo, CA). Briefly, a single apoprotein ΔBCΔBCCP *Re*PC crystal was pulverized in

*Biochemical and Biophysical Research Communications*, Vol. 441, No. 2 (November 2013): pg. 377-382. DOI. 

500 µL of precipitant solution and 0.5 µL of the seed solution was added to the crystallization drop immediately following mixing. The drop was covered with paraffin oil and diamond shaped crystals formed with 2–3 days. After 5–7 days, the crystals were serially transferred in 5% (v/v) glycerol increments from a synthetic mother liquor solution consisting of 11% (w/v) PEG 8000, 70 mM BisTris (pH 6.0), 275 mM TMACl, 5% (v/v) glycerol, and 25 mM oxalate to a cryoprotectant solution consisting of 11.5% (w/v) PEG 8000, 90 mM BisTris (pH 6.0), 300 mM TMACl, 20% (v/v) glycerol, and 25 mM oxalate and flash cooled in liquid nitrogen.

### *ΔBCΔBCCP RePC with 3-bromopyruvate or 3-hydroxypyruvate*

Ligand soaking was necessary to obtain the structures of ΔBCΔBCCP *Re*PC with 3-bromopyruvate or 3-hydroxypyruvate. The protein solution consisting of 12.2 mg/mL ΔBCΔBCCP *Re*PC, was mixed at a 1:1 ratio with the precipitant solution comprised of 11.3% (w/v) PEG 8000, 99 mM BisTris (pH 6.0), and 346 mM TMACl. The crystallization drop was seeded and covered with paraffin oil as described above. Apo crystals of ΔBCΔBCCP *Re*PC were transferred and soaked in a mother liquor solution containing 10% (w/v) PEG 8000, 80 mM BisTris (pH 6.0), 200 mM TMACl, and 80 mM 3-bromopyruvate for 16 hours at room temperature. Similarly, apo crystals of ΔBCΔBCCP *Re*PC with 3-hydroxypyruvate were transferred and soaked in an identical mother liquor solution for 24 hours with 130 mM 3-hydroxypyruvate in place of 3-bromopyruvate. Crystals were then serially transferred in 5% (v/v) glycerol increments from the synthetic mother liquor solution to a cryoprotectant solution consisting of 11% (w/v) PEG 8000, 90 mM BisTris (pH 6.0), 200 mM TMACl, 80 mM 3-bromopyruvate or 130 mM 3-hydroxypyruvate, and 20% (v/v) glycerol and flash cooled in liquid nitrogen.

## *Data Collection, Structure Determination, and Refinement*

X-ray diffraction data were collected at the Advanced Photon Source (APS, Argonne, IL), beamline LS-CAT (Life Sciences Collaborative Access Team) 21-ID-G and 21-ID-F on Rayonix MarMosaic 300 CCD and 225 CCD detectors, respectively. The

*Biochemical and Biophysical Research Communications*, Vol. 441, No. 2 (November 2013): pg. 377-382. DOI. 

wavelength for all structures was tuned to 0.979 Å and the diffraction images were processed with the HKL2000 suite [8]. The structures were solved by molecular replacement using the structure of ΔBCΔBCCP *Re*PC (pdb i.d. 4JX4) as the search model with the program Phaser [9]. Following molecular replacement, translation/liberation/screw (TLS) refinements were performed using REFMAC [10]. Each monomer was treated as a rigid TLS group. All four monomers in the asymmetric unit were restrained using noncrystallographic symmetry for all models during the entire refinement process. The models were extended by several rounds of manual model building with COOT [11] and successive refinements with REFMAC. Water molecules were added to the models in COOT with subsequent manual verification. Data collection and processing statistics are summarized in Table 1. The atomic coordinates for ΔBCΔBCCP *Re*PC with oxalate, ΔBCΔBCCP *Re*PC with 3-hydroxypyruvate and ΔBCΔBCCP *Re*PC with 3-bromopyruvate have been deposited in the Protein Data Bank as entry 4MFD, 4MFE and 4MIM, respectively.

**Table 1**
Data collection and refinement statistics.

| | ΔBCΔBCCP *Re*PC + oxalate | ΔBCΔBCCP *Re*PC + 3-hydroxypyruvate | ΔBCΔBCCP *Re*PC + 3-bromopyruvate |
|---|---|---|---|
| PDB ID code | 4MFD | 4MFE | 4MIM |
| Space group | $P2_12_12_1$ | $P2_12_12_1$ | $P2_12_12_1$ |
| Cell dimensions | | | |
| a, b, c (Å) | 86, 157, 245 | 84, 158, 243 | 86, 157, 243 |
| α, β, γ (°) | 90, 90, 90 | 90, 90, 90 | 90, 90, 90 |
| Resolution range, Å | 50.0–2.55 (2.59–2.55)* | 50.0–2.60 (2.64–2.60)* | 50.0–2.65 (2.70–2.65)* |
| Redundancy | 7.3 (7.1) | 5.5 (5.5) | 7.1 (6.6) |
| Completeness (%) | 99.8 (99.3) | 96.0 (93.2) | 99.9 (99.7) |
| Unique reflections | 108 188 | 91 812 | 95 052 |
| $R_{merge}$ (%) | 8.6 (43.7) | 6.6 (43.4) | 8.2 (44.3) |
| Average I/σ | 21.1 (4.4) | 22.8 (3.3) | 24.5 (3.6) |
| Refinement: | | | |
| Resolution range, Å | 48.26–2.55 (2.61–2.55) | 49.37–2.61 (2.67–2.61) | 48.13–2.65 (2.72–2.65) |
| $R_{cryst}$ | 0.193 (0.262) | 0.177 (0.238) | 0.186 (0.279) |
| $R_{free}$ | 0.240 (0.296) | 0.225 (0.298) | 0.235 (0.334) |
| No. protein atoms | 17,814 | 17,488 | 17,532 |
| No. water molecules | 190 | 169 | 136 |
| Wilson B-value (Å$^2$) | 51.2 | 59.9 | 53.8 |
| Average total B-factors ($B_{TLS} + B_{residual}$) (Å$^2$) | | | |
| Protein | 78.8 | 78.5 | 76.9 |
| Chain A | 53.2 | 58.4 | 56.0 |
| Chain B | 69.1 | 91.2 | 90.6 |
| Chain C | 101.1 | 74.5 | 73.4 |
| Chain D | 93.5 | 91.2 | 88.7 |
| Ligands | 62.2 | 66.6 | 60.5 |
| Solvent | 49.3 | 56.4 | 54.9 |
| Ramachandran (%) | | | |
| Most favored | 90.9 | 90.4 | 90.8 |
| Additionally allowed | 8.3 | 8.9 | 8.7 |
| Generously allowed | 0.7 | 0.7 | 0.5 |
| Disallowed | 0.0 | 0.0 | 0.0 |
| r.m.s. deviations | | | |
| Bond lengths (Å) | 0.0157 | 0.0156 | 0.0140 |
| Bond angles (°) | 1.638 | 1.727 | 1.612 |

* Values in parentheses are for the highest resolution bin.

*Biochemical and Biophysical Research Communications*, Vol. 441, No. 2 (November 2013): pg. 377-382. DOI. 

# Results and Discussion

## *Structure of the RePC CT domain with an intermediate analogue*

The carboxyl transfer reaction in the CT domain of PC is proposed to proceed through a stabilized enolpyruvate intermediate [2]. In the CT active site, carboxybiotin decarboxylates to release $CO_2$. The resulting biotin enolate abstracts a proton from a nearby conserved threonine (Thr882 in *Re*PC), which, in a concerted step, abstracts a proton from pyruvate to form the enolpyruvate intermediate. The enolpyruvate then attacks the liberated $CO_2$ to form oxaloacetate [2]. The enolpyruvate is typically depicted as being stabilized through bidentate coordination to the Lewis acid metal at the center of the active site and mutations to residues coordinating this metal ion lead to a complete loss of enzymatic activity in PC [12]. However, to date, none of the crystal structures of PC co-crystallized with pyruvate show the substrate chelating the divalent active site metal through a bidentate interaction [3,6,13,14]. Instead, pyruvate is always oriented with just the carbonyl oxygen oriented toward the metal center and, furthermore, a water molecule is often observed to be bridging this interaction.

Oxalate is the most potent inhibitor reported for PC. It is non-competitive with respect to pyruvate with a reported $K_i$ value of 70 μM [15], 50–130 μM [16], and 12 μM [17] for PC enzymes from yeast, rat liver, and chicken liver, respectively. Oxalate is competitive with respect to oxaloacetate and has a dissociation constant of 8.9 μM for the metal center of chicken liver PC [18]. At neutrality, the two carboxylates of oxalate are deprotonated ($pK_{a1}$= 1.19; $pK_{a2}$=4.22) [19]. In this ionization state, oxalate is a strong chelator of metal ions and shares structural and chemical properties with the enolpyruvate intermediate. Typically, enzymes that catalyze reactions proceeding through an enolpyruvate intermediate, such as pyruvate kinase and phosphoenolpyruvate caboxykinase, are observed to bind oxalate as a bidentate ligand in the crystal structures [20–22].

A truncated construct of *Re*PC was generated that lacked both the BC and BCCP domains and included only the allosteric and CT

*Biochemical and Biophysical Research Communications*, Vol. 441, No. 2 (November 2013): pg. 377-382. DOI. 

domains of the enzyme (ΔBCΔBCCP *Re*PC; [5]). Using isothermal titration calorimetry (ITC), the $K_D$ values for pyruvate and oxalate with ΔBCΔBCCP *Re*PC were determined to be ~ 2 mM and 0.13 mM, respectively. These data indicate that oxalate binds the active site with a 15-fold greater affinity than the *bona fide* substrate, pyruvate. To gain further insights into the catalytic mechanism in the CT domain of PC, this construct was co-crystallized with oxalate in order to probe the binding orientation of an enolpyruvate intermediate analogue in the active site of the CT domain.

As previously reported, ΔBCΔBCCP *Re*PC crystallizes in the $P2_12_12_1$ space group and the asymmetric unit is composed of four monomers in a dimer of dimers arrangement [5]. For all structures reported here, all monomers within each asymmetric unit are near identical to one another with the highest r.m.s. deviation for all atoms being 0.3 Å. The CT domain architecture consists of a canonical $\alpha_8\beta_8$ TIM barrel fold with a large C-terminal funnel, comprised of nine α-helices, that leads into the active site at the mouth of the barrel. The active site is centered on the structurally conserved Lewis acid metal, which is either $Mn^{2+}$ or $Zn^{2+}$ [5].

Surprisingly, oxalate does not directly interact with the active site metal ion: the distance between the metal ion and oxalate is 4.5 Å, with a bridging water molecule located 2.3 Å away from the metal (Figure 2A). Instead, it is positioned in the active site similarly to the substrates pyruvate (green; pdb i.d. 4JX5) and oxamate (yellow; pdb i.d. 4LOC) (Figure 2B). The planes of the carboxyl moieties for oxalate are staggered such that one carboxyl moiety forms a salt bridge with the guanidinium side-chain of Arg621 and the other maintains hydrogen bond interactions with Arg548 (3.1 Å) and Gln552 (3.3 Å), two residues that are essential for *Re*PC catalysis [4]. Pyruvate and oxamate also interact with Arg621, Arg548 and Gln552, but they adopt a planar conformation in the active site of *Re*PC ([5]; pdb i.d. 4LOC). Because the planes of the oxalate carboxyl moieties are staggered, the carboxyl moiety closest to the metal center is positioned near to Thr882, the residue responsible for transferring a proton to the enolpyruvate intermediate in the oxaloacetate decarboxylation reaction. Additionally, the binding of oxalate appears to be specific, since it promotes a substrate-induced closure of the

*Biochemical and Biophysical Research Communications*, Vol. 441, No. 2 (November 2013): pg. 377-382. DOI. 

active site through an interaction between the hydroxyl moiety of Tyr628 and the side chain of Asp590 [5].

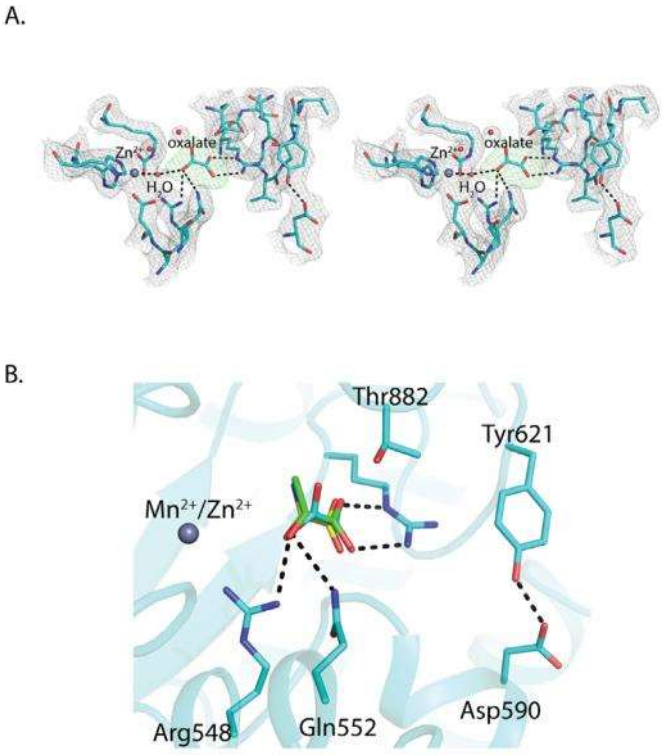


**Figure 2** A. Stereo view of representative electron density for the active site of ΔBCΔBCCP *Re*PC co-crystallized with oxalate. The $2F_o$-$F_c$ electron density map is contoured at 1.0 σ and is represented as a grey mesh. The $F_o$-$F_c$ omit density map is contoured at 3.0 σ and is represented as a green mesh. B. Structural overlay of ΔBCΔBCCP *Re*PC with oxalate (cyan; monomer A) against the structures of ΔBCΔBCCP *Re*PC with pyruvate (green; pdb i.d. 4JX5 - monomer A) and oxamate (yellow; pdb i.d. 4LOC - monomer A). The rms deviation of the structure with oxalate against the structures with pyruvate and oxamate is 0.17 and 0.20 Å, respectively.

The structure of ΔBCΔBCCP *Re*PC with oxalate bound in the active site further clarifies the chemical mechanism in the CT domain of PC. Despite being an excellent metal chelator, oxalate does not form a bidentate interaction with the metal ion located at the center of the active site. This strongly suggests that the enolpyruvate intermediate formed during catalysis is *not* primarily stabilized through an interaction with the metal center. Instead, the developing negative charge in the enolpyruvate intermediate is stabilized through a salt bridge interaction with the guanidinium of Arg621 and interactions with Arg548, Gln552, and the metal. Mutating Arg548 and Gln552 in

*Biochemical and Biophysical Research Communications*, Vol. 441, No. 2 (November 2013): pg. 377-382. DOI. 

*Re*PC results in the complete loss of pyruvate carboxylation activity, further supporting a role for these amino acids in catalysis [4]. Notably, the glutamine/arginine pair (Arg548/Gln552) is conserved in the broader DRE-TIM metalloenzyme family that catalyzes carbon-carbon bond cleavage on substrates that proceed through stabilization of an enolate intermediate [23]. As opposed to a bidentate interaction with the metal ion, the binding orientation adopted by pyruvate and oxalate permits free rotation about the C1–C2 bond to allow C3 to be properly positioned for proton transfer between C3 and the hydroxyl moiety of Thr882 and to orient the carbanion at C3 to attack the liberated $CO_2$ from biotin. Interestingly, the only available structures of a homologous enzyme with bound products and substrates are from the 5S subunit of transcarboxylase, which also revealed that the substrates and products do not directly interact with the active site metal ion [24].

## *Structures of the CT domain from RePC with product analogues*

To date, attempts at capturing structures of oxaloacetate, the reaction product, in the active site of PC have been unsuccessful [6]. Both co-crystallization and soaking attempts with oxaloacetate have resulted in electron density corresponding to pyruvate in the active site ([6]). Capturing structures of oxaloacetate in the active site is complicated by the ability of the CT domain to catalyze the decarboxylation of oxaloacetate [5]. In order to gain insights into how oxaloacetate is positioned in the active site of PC, apo crystals of ΔBCΔBCCP *Re*PC were soaked with 3-hydroxypyruvate and 3-bromopyruvate, structural mimics of oxaloacetate and inhibitors of the carboxyl transfer reaction.

3-hydroxypyruvate, which is a non-competitive inhibitor with respect to MgATP ($K_i$ = 5.5 mM), $HCO_3^-$ ($K_i$ = 7.1 mM), and pyruvate ($K_i$ = 5.4 mM) for the pyruvate carboxylation reaction from *Thiobacillus novellus* PC [25,26], binds in the active site of ΔBCΔBCCP *Re*PC in a similar orientation to pyruvate. Like pyruvate, the carboxyl moiety of 3-hydroxypyruvate forms a salt bridge interaction with the guanidinium moiety of Arg621, while the C2 carbonyl oxygen is within hydrogen bonding distance to the side chains of Arg548 and Gln552

*Biochemical and Biophysical Research Communications*, Vol. 441, No. 2 (November 2013): pg. 377-382. DOI. 

(Figure 3A). Interestingly, the hydroxyl moiety at C3 of 3-hydroxypyruvate is positioned in close proximity to the side chain of Thr882. The position occupied by the hydroxyl moiety is likely to represent the position at which enolpyruvate is carboxylated during the reaction. Like pyruvate, oxamate, and oxalate [5,6]; pdb i.d. 4LOC), 3-hydroxypyruvate is not a bidentate ligand and the binding of 3-hydroxpyruvate promotes the closed conformation of the active site.

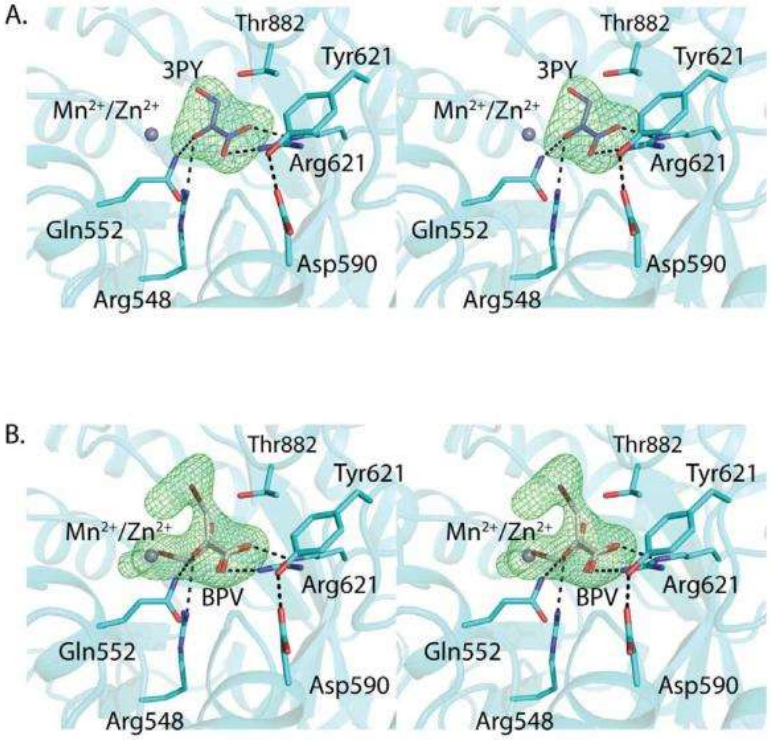


**Figure 3** Representative omit maps for (A) 3-hydroxypyruvate (3PY; purple) and (B) 3-bromopyruvate (BPV; grey) in the active site of ΔBCΔBCCP *Re*PC. The electron density maps are contoured at 3.0 σ.

Halogenating the C3 position of pyruvate results in effective, specific inhibitors of PC (reviewed in [27]). For instance, fluoropyruvate is a non-competitive inhibitor with respect to pyruvate ($K_i$ = 0.17 mM) for the pyruvate carboxylation reaction [17], with pulse NMR data suggesting that it prevents pyruvate coordination in the active site [18]. Further, 10 mM fluoropyruvate and chloropyruvate inhibit gluconeogenesis by 85% and >95%, respectively, in the rat liver by modulating PC activity [28]. Given that halogenated

*Biochemical and Biophysical Research Communications*, Vol. 441, No. 2 (November 2013): pg. 377-382. DOI. 

derivatives of pyruvate are potent inhibitors of PC, we determined the structure of ΔBCΔBCCP *Re*PC with 3-bromopyruvate.

3-bromopyruvate binds in the active site of ΔBCΔBCCP *Re*PC in a similar manner to 3-hydroxypyruvate (Figure 3B). The carboxyl moiety of 3-bromopyruvate forms a salt bridge interaction with the guanidinium moiety of Arg621, and the bromine atom is positioned towards the side-chain of Thr882, much like the C3 hydroxyl moiety of 3-hydroxypyruvate. However, a weaker binding orientation for 3-brompyruvate, modeled at 0.2 occupancy, results in the bromine atom being positioned 2.3 Å away from the active site metal. Normally, the active site metal is octahedrally coordinated by the side chains of Asp549, His747, His749, carbamylated Lys718 and a water molecule. In this second binding mode, 3-bromopyruvate displaces the water molecule and directly interacts with the metal center. This interaction may explain the enhanced potency of halogenated pyruvate derivatives for PC.

3-bromopyruvate has been described as an anti-cancer agent with a wide range of possible targets required for energy metabolism in tumor cells [29]. Most recently, 3-bromopyruvate has also been described as a novel antifungal agent against human pathogens such as *Cryptococcus neoformans* [30]. While it is recognized that 3-bromopyruvate targets multiple metabolic pathways, to our knowledge PC has not been recognized as a specific target for 3-bromopyruvate. Based on the current findings, PC inhibition should be considered when interpreting the mechanism of cellular inhibition for 3-bromopyruvate and other halogenated derivatives of pyruvate.

In summary, we report three X-ray crystal structures of the *Re*PC CT domain with the bound inhibitors oxalate, 3-hydroxypyruvate, and 3-bromopyruvate. Oxalate, which may be considered an analogue of the enolpyruvate reaction intermediate, does not form a bidentate interaction with the active site metal, contrary to what has long been assumed for intermediate stabilization in PC. Instead, the enolpyruvate intermediate is stabilized through a positively charged pocket that includes interactions with Arg621, Arg548, Gln552 in addition to the active site metal. Further, 3-hydroxypyruvate and 3-bromopyruvate, mimcs of the reaction product oxaloacetate, are positioned in the active site such that the C3 bromo/hydroxyl moiety faces the side

*Biochemical and Biophysical Research Communications*, Vol. 441, No. 2 (November 2013): pg. 377-382. DOI. 

chain of Thr882. This positioning strongly suggests that the substrate maintains its orientation in the active site as catalysis proceeds. Two binding modes are suggested in the structure of 3-bromopyruvate. The altered positioning relative to the active site metal may explain the increased inhibition potency of halogenated pyruvate derivatives for PC and demonstrates that PC may factor into the anti-tumor and anti-fungal mechanism of 3-bromopyruvate.

## Highlights

- Structures of pyruvate carboxylase were determined in the presence of three ligands
- Unexpectedly, none of the ligands directly coordinate the active site metal ion
- Structures suggest that substrate orientation remains fixed throughout catalysis
- 3-Bromopyruvate binds in the active site of pyruvate carboxylase

## Acknowledgements

This work was supported by the National Institute of Health grant GM070455 to W.W. Cleland, John C. Wallace, Paul V. Attwood and Martin St. Maurice. Adam D. Lietzan is supported by a Schmitt fellowship from the Arthur J. Schmitt Foundation. Use of the Advanced Photon Source was supported by U.S. Department of Energy, Office of Science, Office of Basic Energy Sciences, under contract No. DE-AC02-06CH11357. Use of the LS-CAT Sector 21 was supported by the Michigan Economic Development Corporation and the Michigan Technology Tri-Corridor for the support of this research program (Grant 085P1000817). The ITC experiments for ΔBCΔBCCP *Re*PC with oxalate and pyruvate were performed on a microcal iTC200 by Verna Frasca at GE Healthcare Life Sciences.

## Abbreviations

| | |
|---|---|
| APS | Advanced Photon Source |
| BC | biotin carboxylase |
| BCCP | biotin carboxyl carrier protein |
| BisTris | 2-[Bis(2-hydroxyethyl)amino]-2-hydroxymethyl)propane-1,3-diol |
| CT | carboxyl transferase |
| LS-CAT | Life Sciences Collaborative Access Team |
| PC | pyruvate carboxylase |

| | |
|---|---|
| PEG | poly(ethylene glycol) |
| *Re*PC | *Rhizobium etli* pyruvate carboxylase |
| *Sa*PC | *Staphylococcus aureus* pyruvate carboxylase |
| TMACl | tetramethylammonium chloride |

**Footnotes**



## References

[1] Jitrapakdee S, St. Maurice M, Rayment I, Cleland WW, Wallace JC, Attwood PV. Structure, mechanism and regulation of pyruvate carboxylase. Biochem. J. 2008;413:369–387.

[2] Zeczycki TN, St. Maurice M, Jitrapakdee S, Wallace JC, Attwood PV, Cleland WW. Insight into the carboxyl transferase domain mechanism of pyruvate carboxylase from *Rhizobium etli*. Biochemistry. 2009;48:4305–4313.

[3] Yu LP, Xiang S, Lasso G, Gil D, Valle M, Tong L. A symmetrical tetramer for *S. aureus* pyruvate carboxylase in complex with coenzyme A. Structure. 2009;17:823–832.

[4] Duangpan S, Jitrapakdee S, Adina-Zada A, Byrne L, Zeczycki TN, St. Maurice M, Cleland WW, Wallace JC, Attwood PV. Probing the catalytic roles of Arg548 and Gln552 in the carboxyl transferase domain of the *Rhizobium etli* pyruvate carboxylase by site-directed mutagenesis. Biochemistry. 2010;49:3296–3304.

[5] Lietzan AD, St. Maurice M. A substrate-induced biotin binding pocket in the carboxyl transferase domain of pyruvate carboxylase. J. Biol. Chem. 2013;288:19915–19925.

[6] Xiang S, Tong L. Crystal structures of human and *Staphylococcus aureus* pyruvate carboxylase and molecular insights into the carboxyltransfer reaction. Nat. Struct. Mol. Biol. 2008;15:295–302.

[7] Yu LP, Chou CY, Choi PH, Tong L. Characterizing the importance of the biotin carboxylase domain dimer for *S. aureus* pyruvate carboxylase catalysis. Biochemistry. 2013;52:488–496.

[8] Otwinowski Z, Minor W. Processing of X-ray diffraction data collected in oscillation mode. Method Enzymol. 1997;276:307–326.

[9] McCoy AJ, Grosse-Kunstleve RW, Adams PD, Winn MD, Storoni LC, Read RJ. Phaser crystallographic software. J. Appl. Crystallogr. 2007;40:658–674.

[10] Winn MD, Murshudov GN, Papiz MZ. Macromolecular TLS refinement in REFMAC at moderate resolutions. Methods Enzymol. 2003;374:300–321.

[11] Emsley P, Cowtan K. Coot: model-building tools for molecular graphics, Acta Crystallogr. D Biol. Crystallogr. 2004;60:2126–2132.

[12] Yong-Biao J, Islam MN, Sueda S, Kondo H. Identification of the catalytic residues involved in the carboxyl transfer of pyruvate carboxylase. Biochemistry. 2004;43:5912–5920.

[13] St. Maurice M, Reinhardt L, Surinya KH, Attwood PV, Wallace JC, Cleland WW, Rayment I. Domain architecture of pyruvate carboxylase, a biotin-dependent multifunctional enzyme. Science. 2007;317:1076–1079.

[14] Lietzan AD, Menefee AL, Zeczycki TN, Kumar S, Attwood PV, Wallace JC, Cleland WW, St. Maurice M. Interaction between the biotin carboxyl carrier domain and the biotin carboxylase domain in pyruvate carboxylase from *Rhizobium etli*. Biochemistry. 2011;50:9708–9723.

[15] Ruiz-Amil M, De Torrontegui G, Palacian E, Catalina L, Losada M. Properties and function of yeast pyruvate carboxylase. J. Biol. Chem. 1965;240:3485–3492.

[16] McClure WR, Lardy HA, Wagner M, Cleland WW. Rat liver pyruvate carboxylase. II. Kinetic studies of the forward reaction. J. Biol. Chem. 1971;246:3579–3583.

[17] Scrutton MC, Olmsted MR, Utter MF. Pyruvate carboxylase from chicken liver. Methods Enzymol. 1969;13:235–249.

[18] Mildvan AS, Scrutton MC, Utter MF. Pyruvate carboxylase. VII. A possible role for tightly bound manganese. J. Biol. Chem. 1966;241:3488–3498.

[19] Riemenschneider W, Tanifuji M. Ullmann's Encyclopedia of Industrial Chemistry. Wiley-VCH Verlag GmbH & Co. KGaA; 2000. Oxalic Acid.

[20] Larsen TM, Benning MM, Rayment I, Reed GH. Structure of the bis(Mg2+)-ATP-oxalate complex of the rabbit muscle pyruvate kinase at 2.1 Å resolution: ATP binding over a barrel. Biochemistry. 1998;37:6247–6255.

[21] Tari LW, Matte A, Pugazhenthi U, Goldie H, Delbaere LT. Snapshot of an enzyme reaction intermediate in the structure of the ATP-Mg2+-oxalate ternary complex of *Escherichia coli* PEP carboxykinase. Nat. Struct. Biol. 1996;3:355–363.

[22] Cotelesage JJ, Prasad L, Zeikus JG, Laivenieks M, Delbaere LT. Crystal structure of *Anaerobiospirillum succiniciproducens* PEP carboxykinase reveals an important active site loop, Int. J. Biochem. Cell Biol. 2005;37:1829–1837.

[23] Forouhar F, Hussain M, Farid R, Benach J, Abashidze M, Edstrom WC, Vorobiev SM, Xiao R, Acton TB, Fu Z, Kim JJ, Miziorko HM, Montelione GT, Hunt JF. Crystal structures of two bacterial 3-hydroxy-3-methylglutaryl-CoA lyases suggest a common catalytic mechanism among a family of TIM barrel metalloenzymes cleaving carbon-carbon bonds. J. Biol. Chem. 2006;281:7533–7545.

[24] Hall PR, Zheng R, Antony L, Pusztai-Carey M, Carey PR, Yee VC. Transcarboxylase 5S structures: assembly and catalytic mechanism of a multienzyme complex subunit. EMBO J. 2004;23:3621–3631.

[25] Charles AM, Willer DW. Pyruvate carboxylase from *Thiobacillus novellus*: properties and possible function. Can. J. Microbiol. 1984;30:532–539.

[26] Charles AM, Willer DW, Scharer JM. Possible regulation of pyruvate carboxylase from *Thiobacillus novellus* by hydroxypyruvate. Curr. Microbiol. 1984;10:265–268.

[27] Zeczycki TN, St. Maurice M, Attwood PV. Inhibitors of pyruvate carboxylase. Open Enzym. Inhib. J. 2010;3:8–26.

[28] Doedens D, Ashmore J. Inhibition of pyruvate carboxylase by chloropyruvic acid and related compounds. Biochem. Pharmacol. 1972;21:1745–1751.

[29] Shoshan MC. 3-bromopyruvate: Targets and outcomes. J. Bioenerg. Biomembr. 2012;44:7–15.

[30] Dylag M, Lis P, Niedzwiecka K, Ko YH, Pedersen PL, Goffeau A, Ulaszewski S. 3-Bromopyruvate: A novel antifungal agent against the human pathogen Cryptococcus neoformans, Biochem. Biophys. Res. Commun. 2013;434:322–327.